AN ADAPTIVE WOOD COMPOSITE: THEORY

Watanachai Smittakorn
Graduate Student

and

Paul R. Heyliger
Professor
Department of Civil Engineering
Colorado State University
Fort Collins, CO 80523

(Received September 2000)

ABSTRACT

A theoretical model is presented for the steady-state and transient behavior of adaptive wood composite plates composed of layers of wood and other piezoelectric materials. Effects of the mechanical, electrical, temperature, and moisture fields are studied simultaneously using a discrete-layer model of the governing equations. These are solved using the finite element method. The computational model employs a one-dimensional Lagrange linear interpolation function in the through-thickness direction and two-dimensional quadratic finite element for the in-plane approximations, treating the displacements, potential, temperature, and moisture as the nodal unknowns. Representative examples of adaptive wood composites are modeled and potential applications are discussed.

Keywords: Adaptive wood composite, laminated plate, hygrothermopiezoelectric effect, discrete-layer model, finite element model.

INTRODUCTION

Widely used composite structures provide significant versatility in allowing structural materials to reach their best performance. Studies of composite wood structures have been discussed by many authors, including in the books by Bodig and Jayne (1982), Breyer (1993), and the references cited therein. Properties and utilization of wood have also been demonstrated by Haygreen and Bowyer (1982), Tsoumis (1991), and Desch and Dinwoodie (1996). However, only purely elastic effects have been the major focus in most studies involving wood. Hygroscopic (moisture) deformation has been considered (Lang et al. 1995; Xu and Suchsland 1996), and other studies regarding wood-cement composites (Mougel et al. 1995), general wood composites (Sharp 1994), and dynamic panel measurements (Rodgers 1991; Schumacher 1988) have all been based on elements of laminated wood mechanics. Problems of wood drying have received a considerable amount of attention from many researchers. The effects of moisture and temperature in wood have been investigated in studies by McMillen (1955), Simpson (1973), Thomas et al. (1980), Morgan et al. (1982), Plumb et al. (1984), Siau (1984), Skaar (1988), Irudayaraj et al. (1990), Cloutier et al. (1992) Cloutier and Fortin (1993), Gui et al. (1994), Choong et al. (1999), and Tremblay et al. (1999).

It is possible for piezoelectric materials, which have the capability of both sensing and actuation, to be integrated into wood composites. This results in what can be termed an "adaptive" (or "intelligent") wood composite structure. The piezoelectric effect is the phenomenon in a material that results in an electric field in response to applied mechanical stress and, conversely, strain in presence of an applied electric field (Voight 1928; Mason 1950; Cady 1964). Wood has also been reported to exhibit some piezoelectric effects

Wood and Fiber Science, 33(4), 2001, pp. 595–608
© 2001 by the Society of Wood Science and Technology

(Fukada 1968; Knuffel and Pizzi 1986). When adaptive wood composites are exposed to changes in environment, temperature and moisture can have significant effects on the structural behavior (Whitney and Ashton 1971; Sih et al. 1986) and need to be taken into account along with the mechanical and electrical effects. Effects of elastic, electric, and temperature fields have been simultaneously studied in thermopiezoelectricity, and the comprehensive generalized theories have been given by Mindlin (1974) and Nowacki (1975). These thermopiezoelectric effects on composite plate structures have been explored in recent years by many researchers (Tauchert 1992; Xu et al. 1995). Smittakorn and Heyliger (2000) have extended this theory to incorporate the effects of moisture.

To analyze the mechanics of wood composite plates, many equivalent-single-layer (ESL) theories in two-dimensions have been developed (Jones 1975; Reddy 1997; Hyer 1998). Among them are the classical lamination theory (CLT), first- and higher-order shear deformation theories. These ESL theories yield very good approximations only when applying to relatively thin plate problems. More accurate results, when needed, can be obtained by employing 3-D theories. Recently, many 3-D theories, both exact and approximate, have been developed for elastic and piezoelectric laminates by Pagano (1970), Pauley and Dong (1976), Reddy (1987, 1989), Ray et al. (1993), Heyliger (1994, 1997), Heyliger et al. (1994) Heyliger and Saravanos (1995), Saravanos et al. (1997), and Lee and Saravanos (1997). However, most of these models do not consider the combined effects of elasticity, moisture, temperature, and electric field. Wood is one of the few materials in which these fields are strongly coupled, and it is the objective of this study to investigate these structures using a new computational model.

In this study, adaptive wood composite structures are investigated through the use of piezoelectric elements in the wood systems in the form of laminated plates. Adaptive elements have the advantage of changing their physical characteristics (primarily dimensions) in the changing environment. Piezoelectric materials allow the composites to achieve the capability of self-monitoring or actuation. Therefore, with piezoelectric elements, the influence of temperature, moisture, and load can be countered or supplemented. Effects of mechanical, electrical, temperature, and moisture fields on the composites are considered simultaneously as hygrothermopiezoelectric media.

Steady-state and transient behavior within the linear range of material response is investigated. Excitations on the laminates can be any one of applied traction, displacement, normal electric displacement, electric potential, normal heat flux, temperature, normal moisture flux, or moisture concentration on the bounding surfaces. A discrete-layer finite element model in three dimensions is developed to yield the approximate solution for the displacement, electric potential, temperature, and moisture concentration in the laminae. Approximation functions (or shape functions) are represented by 1-D finite element functions in the through-thickness direction and 2-D finite element functions in the plane of the laminate. This extends the capability of discrete-layer elements, developed most extensively by Reddy (1987, 1989) to include the effects of moisture, temperature, and piezoelectricity, for the application to wood composites.

GOVERNING EQUATIONS

Based on Mindlin (1974), Nowacki (1975), Sih et al. (1986), Reddy (1997), and Smittakorn and Heyliger (2000), the governing equations in three dimensions for a linear anisotropic hygrothermopiezoelectric medium are defined pointwise in the solid volume of the wood composite, denoted as Ω. We treat the wood as a homogeneous, anisotropic medium in the entirety of this study. All variables introduced in this section are defined in Appendix I.

The equations of motion (conservation of momentum) with the absence of body forces are

$$\sigma_{ij,j} = \rho\ddot{u}_i \qquad (1)$$

Maxwell's equation for electrostatics (conservation of charge) with the absence of free charge is

$$D_{i,i} = 0 \tag{2}$$

The heat conduction equation with the absence of heat source/sink is

$$p_{i,i} = -T_0\dot{\eta} \tag{3}$$

The moisture diffusion equation (conservation of mass of moisture) with the absence of moisture source/sink is

$$q_{i,i} = -\dot{\gamma} \tag{4}$$

The constitutive relations for stress tensor, electric displacement, and entropy density are assumed to be linear and have the following relations:

$$\sigma_{ij} = C_{ijkl}S_{kl} - e_{lij}E_l - \lambda_{ij}\theta - \mu_{ij}\gamma \tag{5}$$

$$D_i = e_{ikl}S_{kl} + \epsilon_{il}E_l + r_i\theta \tag{6}$$

$$\eta = \lambda_{kl}S_{kl} + r_lE_l + \frac{\rho c_v}{T_0}\theta \tag{7}$$

The strain-displacement relations for infinitesimal deformation are given by

$$S_{ij} = \frac{1}{2}(u_{i,j} + u_{j,i}) \tag{8}$$

The relationship between the electric field, E_i, and the electric potential, ϕ, is defined as

$$E_i = -\phi_{,i} \tag{9}$$

The heat flux and moisture flux are assumed to be dependent on the gradients of temperature and moisture as

$$p_i = -\kappa_{ij}\theta_{,j} \tag{10}$$

$$q_i = -\zeta_{ij}\gamma_{,j} \tag{11}$$

where $i, j, k, l = 1, 2, 3$.

Appropriate boundary and initial conditions must be specified in order for a unique solution to exist for the system of partial differential equations. Boundary conditions are specified in the following forms:

$$u_i = \hat{u}_i(x, y, z, t) \quad \text{on } \Gamma_1^{u_i} \tag{12}$$

$$\sigma_{ij}n_j = \hat{t}_i(x, y, z, t) \quad \text{on } \Gamma_2^{u_i} \tag{13}$$

$$\phi = \hat{\phi}(x, y, z, t) \quad \text{on } \Gamma_1^{\phi} \tag{14}$$

$$D_in_i = \hat{D}_n(x, y, z, t) \quad \text{on } \Gamma_2^{\phi} \tag{15}$$

$$\theta = \hat{\theta}(x, y, z, t) \quad \text{on } \Gamma_1^{\theta} \tag{16}$$

$$p_in_i = \hat{p}_n(x, y, z, t) \quad \text{on } \Gamma_2^{\theta} \tag{17}$$

$$\gamma = \hat{\gamma}(x, y, z, t) \quad \text{on } \Gamma_1^{\gamma} \tag{18}$$

$$q_in_i = \hat{q}_n(x, y, z, t) \quad \text{on } \Gamma_2^{\gamma} \tag{19}$$

where the overhat symbol ^ above the variables denotes a specified value or function. $\Gamma_1{}^a$ and $\Gamma_2{}^a$ are parts of the boundary and they constitute the entire solid boundary Γ (i.e., $\Gamma_1{}^a + \Gamma_2{}^a = \Gamma$).

For the transient problem, the initial conditions are specified at time $t = 0$ as follows:

$$u_i = u_i^0(x, y, z) \tag{20}$$

$$\dot{u}_i = \dot{u}_i^0(x, y, z) \tag{21}$$

$$\phi = \phi^0(x, y, z) \tag{22}$$

$$\theta = \theta^0(x, y, z) \tag{23}$$

$$\gamma = \gamma^0(x, y, z) \tag{24}$$

MATHEMATICAL MODEL

Here the mathematical formulation is briefly presented. The conservation Eqs. (1) to (4) are formulated in a weak form using the method of weighted residuals (Reddy 1993) as

$$0 = \int_\Omega [\delta u_i(\sigma_{ij,j} - \rho\ddot{u}_i) + \delta\phi D_{i,i} + \delta\theta(p_{i,i} + T_0\dot{\eta}) + \delta\gamma(q_{i,i} + \dot{\gamma})]\, d\Omega \tag{25}$$

where δu_i, $\delta\phi$, $\delta\theta$, and $\delta\gamma$ are arbitrary and independent weight functions. After integrating by parts, applying the divergence theorem, substituting the constitutive Eqs. (5) to (11), and rewriting the displacement variables using $u_1 = u$, $u_2 = v$, $u_3 = w$, $t_1 = t_x$, $t_2 = t_y$, and $t_3 = t_z$, we reach the final weak form as follows:

$$\int_{\Omega} \delta u \rho \ddot{u}\, d\Omega + \int_{\Omega} \{\nabla \delta u\}^T([C^{xx}]\{\nabla u\} + [C^{xy}]\{\nabla v\} + [C^{xz}]\{\nabla w\} + [e^x]^T\{\nabla \phi\} - \{\lambda^x\}\theta - \{\mu^x\}\gamma)\, d\Omega$$

$$= \oint_{\Gamma} \delta u t_x\, d\Gamma \tag{26}$$

$$\int_{\Omega} \delta v \rho \ddot{v}\, d\Omega + \int_{\Omega} \{\nabla \delta v\}^T([C^{yx}]\{\nabla u\} + [C^{yy}]\{\nabla v\} + [C^{yz}]\{\nabla w\} + [e^y]^T\{\nabla \phi\} - \{\lambda^y\}\theta - \{\mu^y\}\gamma)\, d\Omega$$

$$= \oint_{\Gamma} \delta v t_y\, d\Gamma \tag{27}$$

$$\int_{\Omega} \delta w \rho \ddot{w}\, d\Omega + \int_{\Omega} \{\nabla \delta w\}^T([C^{zx}]\{\nabla u\} + [C^{zy}]\{\nabla v\} + [C^{zz}]\{\nabla w\} + [e^z]^T\{\nabla \phi\} - \{\lambda^z\}\theta - \{\mu^z\}\gamma)\, d\Omega$$

$$= \oint_{\Gamma} \delta w t_z\, d\Gamma \tag{28}$$

$$\int_{\Omega} \{\nabla \delta \phi\}^T([e^x]\{\nabla u\} + [e^y]\{\nabla v\} + [e^z]\{\nabla w\} - [\epsilon]\{\nabla \phi\} + \{r\}\theta)\, d\Omega = \oint_{\Gamma} \delta \phi D_n\, d\Gamma \tag{29}$$

$$\int_{\Omega} \delta \theta T_0\left(-\{\lambda^x\}^T\{\nabla \dot{u}\} - \{\lambda^y\}^T\{\nabla \dot{v}\} - \{\lambda^z\}^T\{\nabla \dot{w}\} + \{r\}^T\{\nabla \dot{\phi}\} - \frac{\rho c_v}{T_0}\dot{\theta}\right) d\Omega$$

$$+ \int_{\Omega} \{\nabla \delta \theta\}^T(-[\kappa]\{\nabla \theta\})\, d\Omega = \oint_{\Gamma} \delta \theta p_n\, d\Gamma \tag{30}$$

$$\int_{\Omega} (-\delta \gamma \dot{\gamma})\, d\Omega + \int_{\Omega} \{\nabla \delta \gamma\}^T(-[\zeta]\{\nabla \gamma\})\, d\Omega = \oint_{\Gamma} \delta \gamma q_n\, d\Gamma \tag{31}$$

where these vectors and matrices were explicitly defined in Smittakorn and Heyliger (2000).

The approximation to the weak form Eqs. (26) to (31) for displacement components (u, v, and w), electric potential (ϕ), temperature change (θ), and moisture change (γ) is sought in the following form:

$$a(x, y, z, t) = \sum_{k=1}^{m_a} \sum_{l=1}^{n_a} N_{kl}^a(x, y, z) a_{kl}(t) = \lfloor N^a(x, y, z) \rfloor \{a(t)\} \tag{32}$$

where the approximation functions (or shape functions) and the corresponding unknown values (or functions) are

$$\lfloor N^a(x, y, z) \rfloor = \lfloor N_{11}^a(x, y, z) \cdots N_{kl}^a(x, y, z) \cdots N_{m_a n_a}^a(x, y, z) \rfloor \tag{33}$$

$$\{a(t)\} = \begin{Bmatrix} a_{11}(t) \\ \vdots \\ a_{kl}(t) \\ \vdots \\ a_{m_a n_a}(t) \end{Bmatrix} \tag{34}$$

and the weight functions are assumed as

$$\delta a = \lfloor N^a(x, y, z) \rfloor^T \tag{35}$$

Here a and δa represent the variables u, v, w, ϕ, θ, and γ and the associated weight functions. In this study, a discrete-layer finite element model is employed. Following the discrete-layer (or layerwise) theory by Reddy (1987, 1989), the approximation functions $N_{kl}^a(x, y, z)$ in three dimensions are separated into products of functions in x-y plane and functions in z-direction (through-thickness direction) using the method of variable separation as

$$N_{kl}^a(x, y, z) = \Psi_k^a(x, y)\Xi_l^a(z) \tag{36}$$

where $\Psi_k^a(x, y)$ is the k-th term of approximation function in x-y plane, and $\Xi_l^a(z)$ is the l-th term of approximation function in z-direction. By using only C^0-continuity of the primary unknowns, these elements have the advantage of being able to model the discontinuity of stress and electric field in the direction through the thickness (see Fig. 1). In this article, identically for all variables u, v, w, ϕ, θ, and γ, the in-plane shape function $\Psi_k(x, y)$ is used as an 8-noded serendipity quadrilateral element, whereas the through-thickness shape function $\Xi_l(z)$ is used as a Lagrange linear element. For more details of these elements and their shape functions see Reddy (1993).

After substituting these functions into the weak form Eqs. (26) to (31), the system of equations can be written in matrix form as

$$\begin{bmatrix} [M^{uu}] & [0] & [0] & [0] & [0] & [0] \\ [0] & [M^{vv}] & [0] & [0] & [0] & [0] \\ [0] & [0] & [M^{ww}] & [0] & [0] & [0] \\ [0] & [0] & [0] & [0] & [0] & [0] \\ [0] & [0] & [0] & [0] & [0] & [0] \\ [0] & [0] & [0] & [0] & [0] & [0] \end{bmatrix} \begin{Bmatrix} \{\ddot{u}\} \\ \{\ddot{v}\} \\ \{\ddot{w}\} \\ \{\ddot{\phi}\} \\ \{\ddot{\theta}\} \\ \{\ddot{\gamma}\} \end{Bmatrix} + \begin{bmatrix} [0] & [0] & [0] & [0] & [0] & [0] \\ [0] & [0] & [0] & [0] & [0] & [0] \\ [0] & [0] & [0] & [0] & [0] & [0] \\ [0] & [0] & [0] & [0] & [0] & [0] \\ [C^{\theta u}] & [C^{\theta v}] & [C^{\theta w}] & [C^{\theta\phi}] & [C^{\theta\theta}] & [0] \\ [0] & [0] & [0] & [0] & [0] & [C^{\gamma\gamma}] \end{bmatrix} \begin{Bmatrix} \{\dot{u}\} \\ \{\dot{v}\} \\ \{\dot{w}\} \\ \{\dot{\phi}\} \\ \{\dot{\theta}\} \\ \{\dot{\gamma}\} \end{Bmatrix}$$

$$+ \begin{bmatrix} [K^{uu}] & [K^{uv}] & [K^{uw}] & [K^{u\phi}] & [K^{u\theta}] & [K^{u\gamma}] \\ [K^{vu}] & [K^{vv}] & [K^{vw}] & [K^{v\phi}] & [K^{v\theta}] & [K^{v\gamma}] \\ [K^{wu}] & [K^{wv}] & [K^{ww}] & [K^{w\phi}] & [K^{w\theta}] & [K^{w\gamma}] \\ [K^{\phi u}] & [K^{\phi v}] & [K^{\phi w}] & [K^{\phi\phi}] & [K^{\phi\theta}] & [0] \\ [0] & [0] & [0] & [0] & [K^{\theta\theta}] & [0] \\ [0] & [0] & [0] & [0] & [0] & [K^{\gamma\gamma}] \end{bmatrix} \begin{Bmatrix} \{u\} \\ \{v\} \\ \{w\} \\ \{\phi\} \\ \{\theta\} \\ \{\gamma\} \end{Bmatrix} = \begin{Bmatrix} \{F^u\} \\ \{F^v\} \\ \{F^w\} \\ \{F^\phi\} \\ \{F^\theta\} \\ \{F^\gamma\} \end{Bmatrix} \tag{37}$$

where the non-zero elements of the matrices $[K]$, $[M]$, and $[C]$, and vector $\{F\}$ here share the general forms of those in Smittakorn and Heyliger (2000). Representative examples of these terms are given in detail in Appendix II. Imposing the boundary conditions and initial conditions allows us to solve for the primary unknowns $\{u\}$, $\{v\}$, $\{w\}$, $\{\phi\}$, $\{\theta\}$, and $\{\gamma\}$. However, for the system of Eq. (37), the method of mode superposition is not applicable due to the lack of the orthogonality properties. Therefore, we choose to employ a direct step-by-step integration using the Newmark beta method, as shown by Bathe (1996), to solve for the time-dependent solutions.

The discrete-layer model developed here is an extension discrete-layer elastic model (see, e.g., Reddy) to take into account the effects of mechanical, electrical, temperature, and moisture fields simultaneously in a multilayered laminated composite plate. The transient behavior of temperature and moisture diffusion in the composite is also incorporated. Approximation functions, employed here as 1-D Lagrange interpolation functions in the through-thickness direction and 2-D finite element functions in the plane of the plate, make this model equivalent to a conventional 3-D finite element model. The discrete-layer model has some advantages over the conventional 3-D model in such a way that some programming procedures can be simplified. However, the discrete-layer model is based on the assumption that each sublayer (of the laminated plate) is homogeneous and has linear properties, without any time, temperature, or moisture varying properties. Also, each lamina is assumed to be perfectly bonded together without any residual effects. The laminated plate structure can have any configuration in x-y plane, as long as the thickness of each sublayer in z-direction is constant. Essential boundary conditions are specified through primary variables: displacement, electric potential, temperature, and moisture concentration. Natural boundary conditions are specified through surface traction, normal electric displacement, normal heat flux, and normal moisture flux. In our model, since C^0-continuity is required between sublayers, only the primary unknowns are continuous functions. The secondary unknowns of stresses, electric displacement, heat flux, and moisture flux are not continuous at the sublayer interfaces. Therefore, these values, when needed, are computed only at mid-level of each sublayer, and the values elsewhere are calculated by interpolation or extrapolation.

NUMERICAL EXAMPLES AND DISCUSSION

Similar to many structural materials, one major concern in using wood as structural elements is that wood material has a tendency to expand or contract in a changing environment, particularly changes in temperature and moisture. Thus, the wood drying (or soaking) problem has received a considerable amount of attention from structural engineers. However, this model yields an improvement over some earlier studies in that the differing material properties for each layer are all taken into account. In addition, the model allows for the application of an electric field to further change the shape of the wood composite.

In this section, problems of an adaptive wood composite plate, composed of wood and piezoelectric material, subject to the changes in temperature and moisture are simulated. Both steady-state and transient behaviors of the laminate are investigated. The response of interest is the out-of-plane deflection or warping of the plate. Also, the piezoelectric effect is examined in order to evaluate the potential use of the piezoelectric material as a distributed actuator in the composite. Throughout this study, we choose to represent the wood material with walnut species (Bodig and Jayne 1982; Haygreen and Bowyer 1982; Tsoumis 1991; Desch and Dinwoodie 1996; Siau 1984; Choong et al. 1999), and piezoelectric material with PZT4 (Smittakorn and Heyliger 2000).

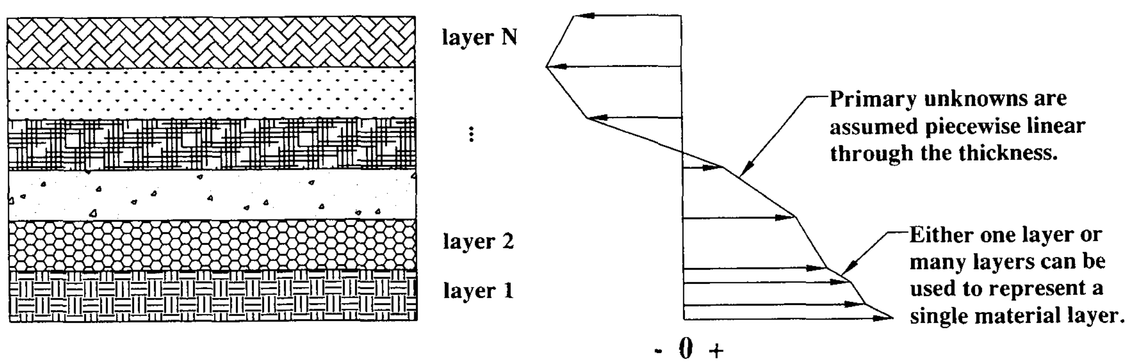

FIG. 1. Discrete-layer model in the through-thickness direction.

These materials are assumed to have the properties shown in Table 1. Voltage is applied to the piezoelectric layer, and deflections are analyzed. We can then visualize how much the piezoelectric layer can counterbalance the warping caused by temperature and moisture changes. In our analyses, the piezoelectric effect of the wood material is ignored since its effect is three orders of magnitude smaller than that of the piezoelectric material (PZT4) used in these examples.

Steady-state response

A 50-mm by 50-mm composite laminate with a layer of wood 6 mm thick on the bottom and a layer of PZT4 0.5 mm thick on the top is examined under three types of steady-state excitations: applied moisture, temperature, and voltage. The boundary conditions of the laminate, for the mechanical variables, used in all these cases are treated as traction-free boundary conditions. Effects of environmental conditions on the deflection of the laminate are simulated in the first and second cases. A unit value of moisture and temperature change is assumed as a representation. In the first case, a simulated change in moisture concentration of 1.0 kg/m^3 is applied at the top and bottom surfaces of the laminate while the temperature at these surfaces is kept constant. In the second case, a simulated change in temperature of 1.0 K is applied at the top and bottom surfaces of the laminate while the moisture concentration at these surfaces is kept constant. Also, the top and bottom faces of the PZT4 layer are grounded at zero potential. To investigate the capability of piezoelectric actuation on the laminate, we apply an electric field to the PZT4 layer in the third case. The voltage of -200.0 V is applied on the top surface while the bottom face of PZT4 is grounded at zero voltage. The top and bottom surfaces of the laminate are kept at constant temperature and moisture concentration.

The numerical models of the laminate are discretized as six sublayers, three for each material, in the through-thickness direction. Us-

TABLE 1. *Material properties for wood and PZT4. The permittivity of free space is $\epsilon_0 = 8.85 \times 10^{-12}$ F/m.*

Properties	Wood	PZT4
Mass density: (kg/m^3)		
ρ	660.8	7600.0
Specific heat coefficient: (Nm/kgK)		
c_v	1360.0	420.0
Elastic constants: (GPa)		
C_{11}	12.22	139.0
C_{22}	0.6699	139.0
C_{33}	1.273	115.0
C_{44}	0.2432	25.6
C_{55}	0.9846	25.6
C_{66}	0.7182	30.6
C_{12}	0.4682	77.8
C_{13}	0.6872	74.3
C_{23}	0.0905	74.3
Piezoelectric constants: (C/m^2)		
e_{15}	0	12.72
e_{24}	0	12.72
e_{31}	0	-5.20
e_{32}	0	-5.20
e_{33}	0	15.08
Relative permittivities:		
ϵ_{11}/ϵ_0	3.50	1475
ϵ_{22}/ϵ_0	2.33	1475
ϵ_{33}/ϵ_0	2.33	1300
Thermal expansion coefficients: (10^{-6}/K)		
α_1	3.5	2.0
α_2	40.0	2.0
α_3	30.0	2.0
Moisture expansion coefficients: (m^3/kg)		
β_1	0	0
β_2	0.00016	0
β_3	0.00011	0
Pyroelectric coefficients: (C/m^{2}K)		
r_1	0	-0.00025
r_2	0	-0.00025
r_3	0	-0.00025
Thermal conductivity coefficients; (N/sK)		
κ_{11}	0.383	1.8
κ_{22}	0.158	1.8
κ_{33}	0.158	1.8
Moisture diffusivity coefficients: (10^{-12} m^2/s)		
ζ_{11}	1731.0	0.25
ζ_{22}	512.0	0.25
ζ_{33}	525.0	0.25

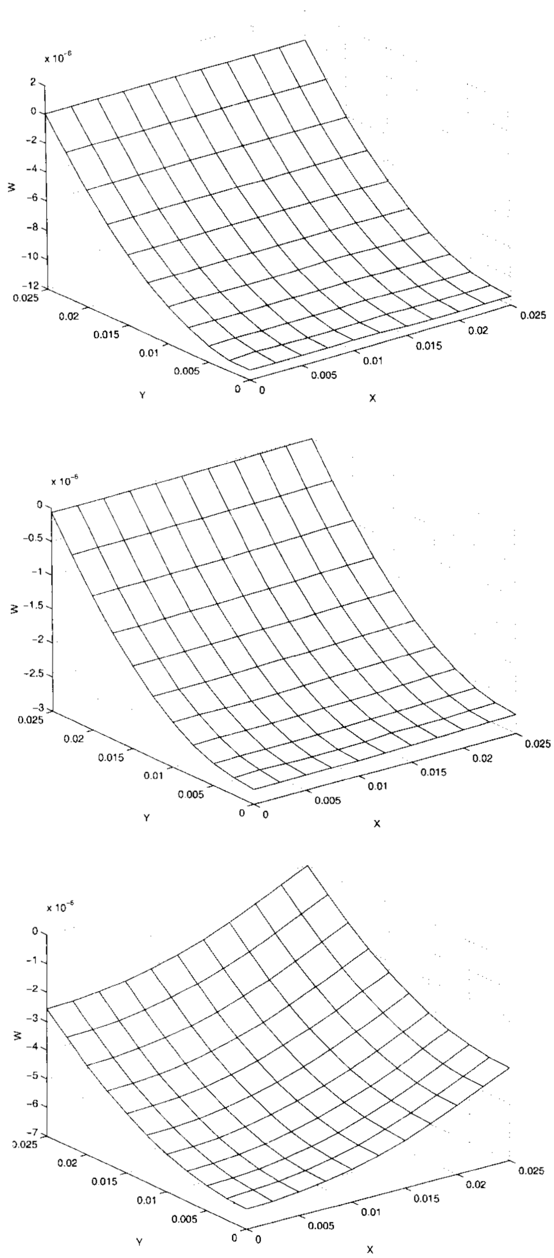

FIG. 2. Deflected shapes of adaptive wood composite plate subject to: (a) applied moisture. (b) applied temperature. (c) applied voltage.

ing the advantage of structural symmetry, a quarter of the domain in x-y plane is modeled. Results of the three cases of steady-state excitation are shown in Fig. 2. Deflected shapes of the laminate subject to the applied moisture, temperature, and voltage are plotted in three dimensions. Deflections on only a quarter of the domain are shown where planes $x = 0$ and $y = 0$ are the planes of symmetry. When subjecting to the changes in moisture (Fig. 2(a)) and temperature (Fig. 2(b)), the composite plate under traction-free boundary conditions behaves similarly to one-way slab structures. This is due to the very high degree of anisotropy in x-y plane for wood material, but low degree for PZT4. However, for a different type of (mechanical) boundary condition (e.g., simple support), the laminate will no longer have only one-way behavior. In Fig. 2(c), the deflected shape of the composite as a response of applied voltage on the piezoelectric layer is plotted. This is to show how much of actuation we can obtain and to see the potential use of the PZT4 as an actuator on wood structures.

To examine the convergence of the numerical models, the in-plane domain is divided into several different grids: 2×2, 3×3, and 4×4. Results from these different discretizations in the x-y plane are shown in Table 2, where the values of the deflection at plate center on the bottom surface ($x = 0$, $y = 0$, $z = 0$) are given. The maximum differences occur when the composite is subjected to the applied voltage. These differences are 0.40% between the 2×2 and 3×3 grids, and 0.22% between 3×3 and 4×4 grids.

Transient response

The laminate studied above is again considered under traction-free boundary conditions, and all the initial conditions are set to be zero. The composite plate is now examined with two types of transient excitations. First, a change of moisture concentration at the top and bottom surfaces of the laminate is applied as bilinear, increased linearly from zero value at time $t = 0$ to 1.0 kg/m^3 at time $t = 20{,}000$ s then kept constant at 1.0 kg/m^3. Temperature at the top and bottom surfaces is kept constant for this case. For the second case, an applied temperature change at the top and bottom sur-

TABLE 2. *Convergence study of adaptive wood composite plate. The maximum values of the deflection are given for the different in-plane discretizations: 2 × 2, 3 × 3, and 4 × 4 elements.*

Cases	2×2	3×3	4×4
Applied moisture ($\times 10^{-5}$ m)	−1.1325	−1.1315	−1.1309
Applied temperature ($\times 10^{-6}$ m)	−2.7815	−2.7791	−2.7775
Applied voltage ($\times 10^{-6}$ m)	−6.3283	−6.3030	−6.2891

faces is increased linearly from zero value at time $t = 0$ to the value of 1.0 K at time $t = 20$ s then kept constant afterward. The moisture concentration at the top and bottom surfaces is kept constant. In both cases, the reference temperature T_0 is assumed as 300.0 K, and the top and bottom surfaces of the PZT4 layer are fixed at zero voltage at all times.

For these transient cases, only one type of discretization of the domain is used for the numerical models. Again with the use of symmetry, the model consists of a quarter of the in-plane domain with four elements (two in x-direction by two in y-direction) and twelve sublayers (six for each material) in the through-thickness z-direction. Transient responses of the laminate to the applied excitations are then calculated using direct step-by-step integration (the constant acceleration method) at each time interval of 1,000 s and 1 s for the cases of applied moisture and applied temperature, respectively. Figure 3 shows the transient responses of the wood laminate at the center point of the plate ($x = 0$, $y = 0$). Deflections at the bottom level ($z = 0$) subject to the applied moisture (Fig. 3(a)) and the applied temperature (Fig. 3(b)) are plotted with time. As the time increases, these transient results converge to the steady-state results. In these graphs, the curvature is changed at the point when the excitation reaches the maximum value ($t = 20{,}000$ s for applied moisture, and $t = 20$ s for applied temperature). The discontinuity of the slope of the applied moisture and temperature is the cause of this. Figure 3(c) shows the moisture variation through the thickness of the laminate at various times for the applied moisture case, and similarly Fig. 3(d) for the temperature variation for the applied temperature case. Wood material has a greater value of moisture diffusivity, but a smaller value of thermal diffusivity than PZT4. Hence the through-thickness plots of moisture and temperature changes show jumps at the interface between the two materials.

CONCLUSIONS

Laminated plates are a well-known form of composite structures. However, when exposed to the environment, the changes in temperature and moisture can cause significant deflections and/or warping in these laminates. This is due to the differences in the material properties, not only in the different kinds of materials, but also in the different directions of an anisotropic material. Wood is one material with a strong influence from anisotropy, moisture, and temperature.

In this research, a piezoelectric material (PZT4) is introduced to form an adaptive wood composite, where the layer of PZT4 can be utilized as a distributed actuator. Deflections caused by the moisture and temperature changes can be controlled or counter-acted by adjusting the electric field applied to the piezoelectric layer. Numerical examples have shown that PZT4 is a possible candidate to be used as an actuator for the wood laminates. Using an applied voltage of 200 V on the given structure, displacements of the order 6×10^{-6} m were generated, which are enough to counter moisture effects of the order 0.5 kg/m^3 or temperature effects of the order 2 K. The piezoelectric effect is instantaneous, and therefore the effect of applied voltage to the composite was demonstrated only for the steady-state case. Moreover, even though the effects of applied moisture, temperature, and electric

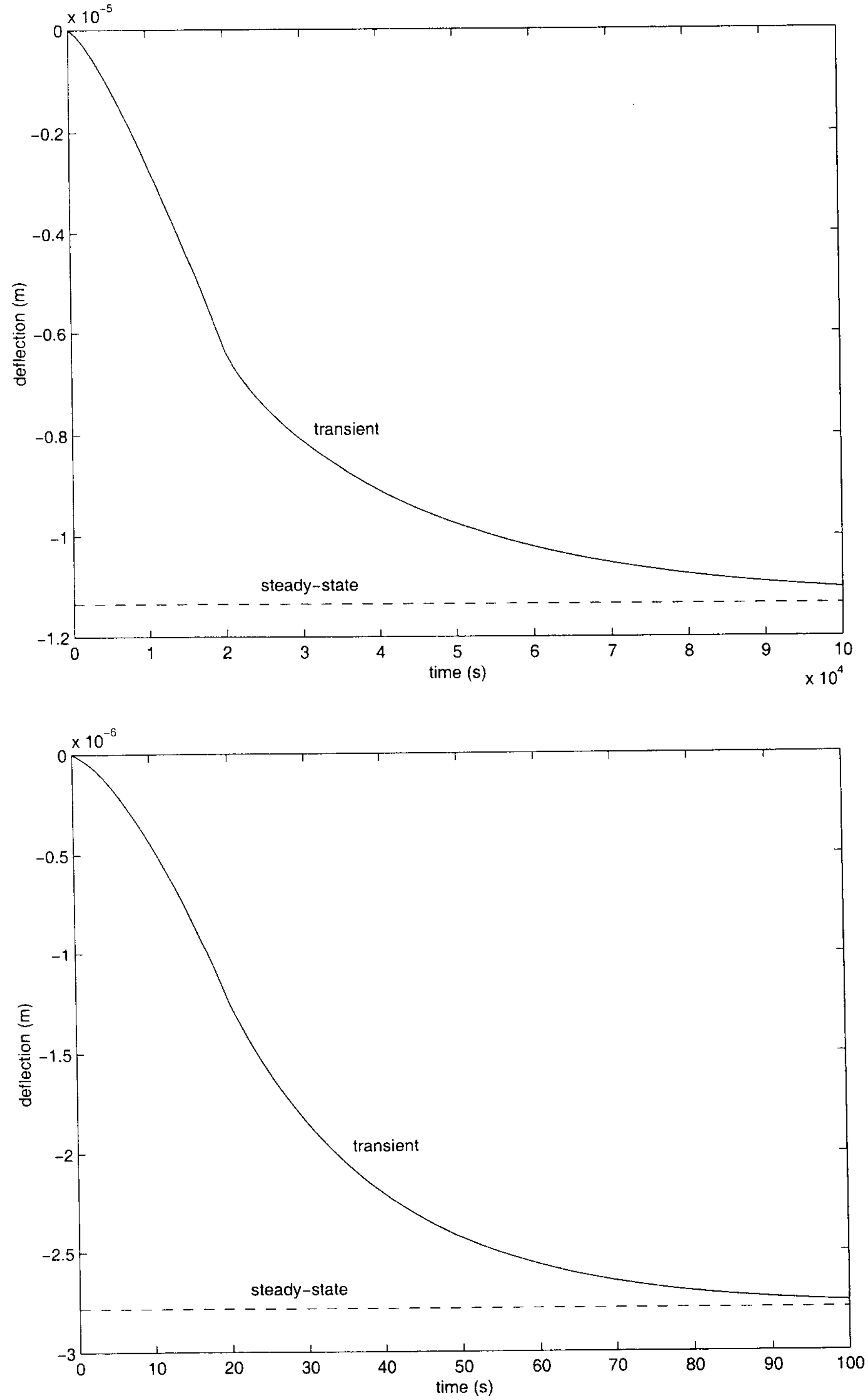

FIG. 3. Transient responses at center of adaptive wood composite plate: (a) transient deflection due to applied moisture. (b) transient deflection due to applied temperature. (c) through-thickness moisture change due to applied moisture. (d) through-thickness temperature change due to applied temperature.

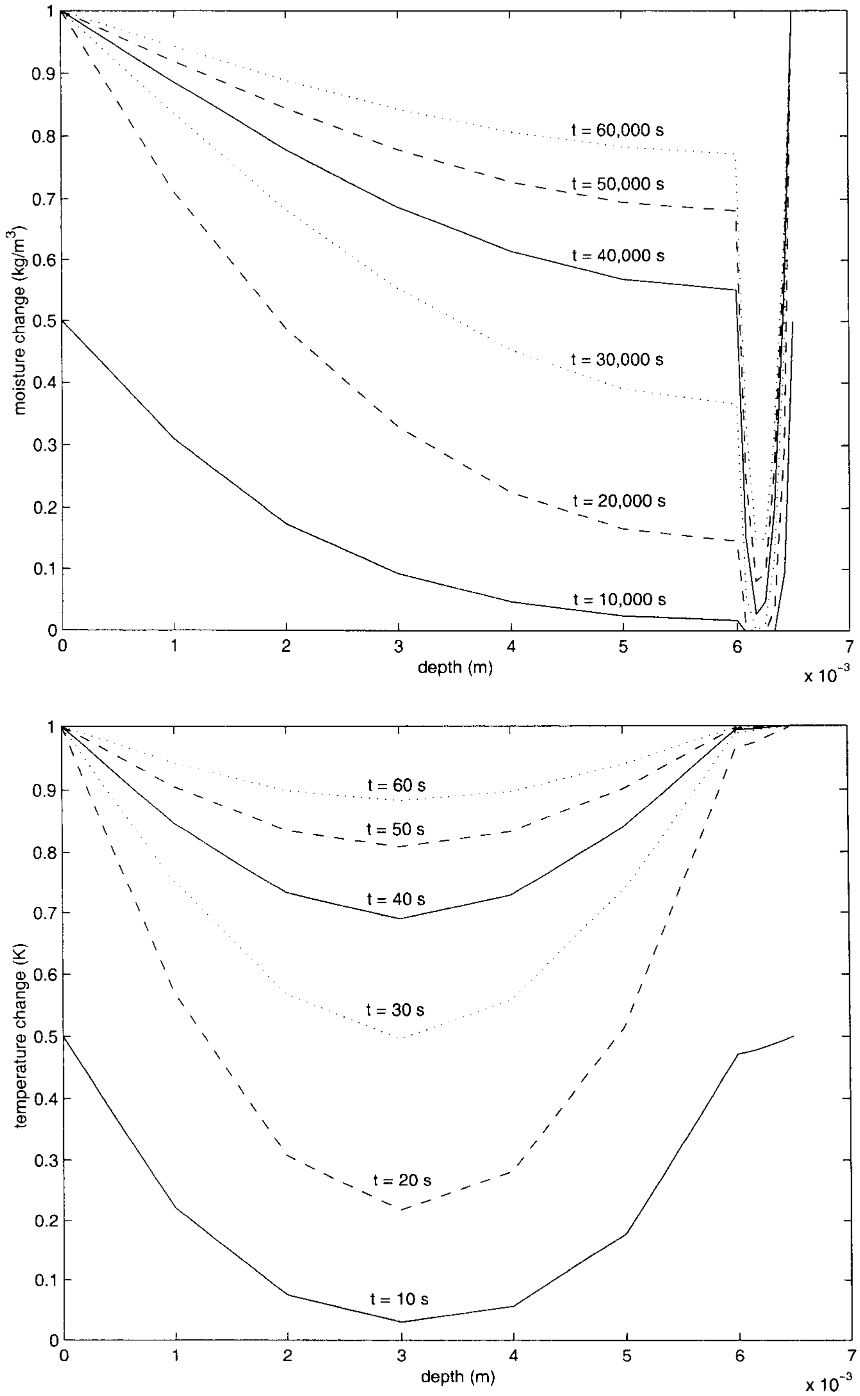

FIG. 3. Continued.

field to the composite are separately shown in the case studies, the combined results of these fields can be easily computed as a linear combination, using the method of superposition. Our results therefore provide an indication of the level of response of adaptive wood composites, and the model provides a means of studying any laminated wood plate where the elastic, temperature, moisture, and electric fields influence the overall structural response. We note here that no experimental verification has been conducted, hence the validity and associated error of the model cannot be determined.

ACKNOWLEDGMENT

This study was supported by Award 9702548 from the NRI Competitive Grants Program of the United States Department of Agriculture. This support is gratefully acknowledged.

APPENDIX I

The nomenclature used in this article is as follows:

σ_{ij} are the components of the stress tensor,
S_{ij} are the components of the infinitesimal strain tensor,
u_i are the components of the displacement,
ρ is the mass density,
D_i are the components of the electric displacement,
E_i are the components of the electric field,
ϕ is the electrostatic potential,
η is the entropy density,
θ is the small temperature change ($\theta = T - T_0$),
T is the absolute temperature,
T_0 is the stress-free reference temperature,
γ is the change of moisture concentration ($\gamma = H - H_0$),
H is the moisture concentration (mass of moisture per unit volume of solid),
H_0 is the stress-free reference moisture concentration,
p_i are the heat flux components,
q_i are the moisture flux components,
C_{ijkl} are the elastic stiffness coefficients,
e_{ikl} are the piezoelectric coefficients,
λ_{ij} are the stress-temperature coefficients ($\lambda_{ij} = C_{ijkl}\alpha_{kl}$),
α_{kl} are the coefficients of thermal expansion,
μ_{ij} are the stress-moisture coefficients ($\mu_{ij} = C_{ijkl}\beta_{kl}$),
β_{kl} are the coefficients of moisture expansion,
ϵ_{il} are the dielectric constants (permittivities),
r_i are the pyroelectric coefficients,
c_v is the specific heat coefficient per unit mass at constant volume,
κ_{ij} are the thermal conductivity coefficients,
ζ_{ij} are the moisture diffusivity coefficients,
n_i are the components of the unit outward normal vector to the bounding surface,
t_i are the surface traction components,
D_n is the normal component of the electric displacement,
p_n is the normal heat flux, and
q_n is the normal moisture flux.

APPENDIX II

Representative examples of the entries in the coefficient matrices can be expressed as

$$M_{pq}^{uu} = M_{ijkl}^{uu} = \int_\Omega \rho\Psi_i\Xi_j\Psi_k\Xi_l \, d\Omega$$

$$C_{pq}^{\theta u} = C_{ijkl}^{\theta u} = -\int_\Omega T_0\Psi_i\Xi_j(\lambda_1\Psi_{k,x}\Xi_l + \lambda_6\Psi_{k,y}\Xi_l + \lambda_5\Psi_k\Xi_{l,z}) \, d\Omega$$

$$C_{pq}^{\theta\phi} = C_{ijkl}^{\theta\phi} = \int_\Omega T_0\Psi_i\Xi_j(r_1\Psi_{k,x}\Xi_l + r_2\Psi_{k,y}\Xi_l + r_3\Psi_k\Xi_{l,z}) \, d\Omega$$

$$C_{pq}^{\theta\theta} = C_{ijkl}^{\theta\theta} = -\int_\Omega \rho c_v\Psi_i\Xi_j\Psi_k\Xi_l \, d\Omega$$

$$C_{pq}^{\gamma\gamma} = C_{ijkl}^{\gamma\gamma} = -\int_\Omega \Psi_i\Xi_j\Psi_k\Xi_l \, d\Omega$$

$$\begin{aligned} K_{pq}^{uu} = K_{ijkl}^{uu} &= \int_\Omega (C_{11}\Psi_{i,x}\Xi_j\Psi_{k,x}\Xi_l + C_{66}\Psi_{i,y}\Xi_j\Psi_{k,y}\Xi_l \\ &\quad + C_{55}\Psi_i\Xi_{j,z}\Psi_k\Xi_{l,z} + 2C_{16}\Psi_{i,x}\Xi_j\Psi_{k,y}\Xi_l \\ &\quad + 2C_{15}\Psi_{i,x}\Xi_j\Psi_k\Xi_{l,z} + 2C_{56}\Psi_{i,y}\Xi_j\Psi_k\Xi_{l,z}) \, d\Omega \end{aligned}$$

$$\begin{aligned} K_{pq}^{u\phi} = K_{ijkl}^{u\phi} &= \int_\Omega (\Psi_{i,x}\Xi_j(e_{11}\Psi_{k,x}\Xi_l + e_{21}\Psi_{k,y}\Xi_l + e_{31}\Psi_k\Xi_{l,z}) \\ &\quad + \Psi_{i,y}\Xi_j(e_{16}\Psi_{k,x}\Xi_l + e_{26}\Psi_{k,y}\Xi_l + e_{36}\Psi_k\Xi_{l,z}) \\ &\quad + \Psi_i\Xi_{j,z}(e_{15}\Psi_{k,x}\Xi_l + e_{25}\Psi_{k,y}\Xi_l + e_{35}\Psi_k\Xi_{l,z}) \, d\Omega \end{aligned}$$

$$K_{pq}^{u\theta} = K_{ijkl}^{u\theta} = -\int_\Omega (\lambda_1\Psi_{i,x}\Xi_j + \lambda_6\Psi_{i,y}\Xi_j + \lambda_5\Psi_i\Xi_{j,z})\Psi_k\Xi_l \, d\Omega$$

$$K_{pq}^{u\gamma} = K_{ijkl}^{u\gamma} = -\int_\Omega (\mu_1\Psi_{i,x}\Xi_j + \mu_6\Psi_{i,y}\Xi_j + \mu_5\Psi_i\Xi_{j,z})\Psi_k\Xi_l \, d\Omega$$

$$K_{pq}^{\phi\phi} = K_{ijkl}^{\phi\phi}$$

$$= -\int_{\Omega} (\epsilon_{11}\Psi_{i,x}\Xi_j\Psi_{k,x}\Xi_l + \epsilon_{22}\Psi_{i,y}\Xi_j\Psi_{k,y}\Xi_l$$

$$+ \epsilon_{33}\Psi_i\Xi_{j,z}\Psi_k\Xi_{l,z} + 2\epsilon_{12}\Psi_{i,x}\Xi_j\Psi_{k,y}\Xi_l$$

$$+ 2\epsilon_{13}\Psi_{i,x}\Xi_j\Psi_k\Xi_{l,z} + 2\epsilon_{23}\Psi_{i,y}\Xi_j\Psi_k\Xi_{l,z})\, d\Omega$$

$$K_{pq}^{\phi\theta} = K_{ijkl}^{\phi\theta} = \int_{\Omega} (r_1\Psi_{i,x}\Xi_j + r_2\Psi_{i,y}\Xi_j + r_3\Psi_i\Xi_{j,z})\Psi_k\Xi_l\, d\Omega$$

$$K_{pq}^{\theta\theta} = K_{ijkl}^{\theta\theta}$$

$$= -\int_{\Omega} (\kappa_{11}\Psi_{i,x}\Xi_j\Psi_{k,x}\Xi_l + \kappa_{22}\Psi_{i,y}\Xi_j\Psi_{k,y}\Xi_l$$

$$+ \kappa_{33}\Psi_i\Xi_{j,z}\Psi_k\Xi_{l,z} + 2\kappa_{12}\Psi_{i,x}\Xi_j\Psi_{k,y}\Xi_l$$

$$+ 2\kappa_{13}\Psi_{i,x}\Xi_j\Psi_k\Xi_{l,z} + 2\kappa_{23}\Psi_{i,y}\Xi_j\Psi_k\Xi_{l,z})\, d\Omega$$

$$K_{pq}^{\gamma\gamma} = K_{ijkl}^{\gamma\gamma}$$

$$= -\int_{\Omega} (\zeta_{11}\Psi_{i,x}\Xi_j\Psi_{k,x}\Xi_l + \zeta_{22}\Psi_{i,y}\Xi_j\Psi_{k,y}\Xi_l$$

$$+ \zeta_{33}\Psi_i\Xi_{j,z}\Psi_k\Xi_{l,z} + 2\zeta_{12}\Psi_{i,x}\Xi_j\Psi_{k,y}\Xi_l$$

$$+ 2\zeta_{13}\Psi_{i,x}\Xi_j\Psi_k\Xi_{l,z} + 2\zeta_{23}\Psi_{i,y}\Xi_j\Psi_k\Xi_{l,z})\, d\Omega$$

REFERENCES

BATHE, K. J. 1996. Finite element procedures. Prentice-Hall, Englewood Cliffs, NJ.

BODIG, J., AND B. A. JAYNE. 1982. Mechanics of wood and wood composites. Van Nostrand Reinhold, New York, NY.

BREYER, D. E. 1993. Design of wood structures. McGraw-Hill, New York, NY.

CADY, W. G. 1964. Piezoelectricity, Rev. ed., vols. I and II. Dover Publications, New York, NY.

CHOONG, E. T., T. F. SHUPE, AND Y. CHEN. 1999. Effect of steaming and hot-water soaking on extractive distribution and moisture diffusivity in southern pine during drying. Wood Fiber Sci. 31(2):143–150.

CLOUTIER, A., AND Y. FORTIN. 1993. A model of moisture movement in wood based on water potential and the determination of the effective water conductivity. Wood Sci. Technol. 27:95–114.

———, ———, AND G. DHATT. 1992. A wood drying finite element model based on the water potential concept. Drying Technol. 10(5):1151–1181.

DESCH, H. E., AND J. M. DINWOODIE. 1996. Timber: Structure, properties, conversion and use, 7th ed. Food Products Press, Binghamton, NY.

FUKADA, E. 1968. Piezoelectricity as a fundamental property of wood. Wood Sci. Technol. 2:299–307.

GUI, Y. Q., E. W. JONES, F. W. TAYLOR, AND C. A. ISSA. 1994. An application of finite element analysis to wood drying. Wood Fiber Sci. 26(2):281–293.

HAYGREEN, J. G., AND J. L. BOWYER. 1982. Forest products and wood science. The Iowa State University Press, Ames, IA.

HEYLIGER, P. R. 1994. Static behavior of laminated elastic/piezoelectric plates. AIAA J. 32:2481–2484.

———. 1997. Exact solutions for simply supported laminated piezoelectric plates. J. Appl. Mech. 64:299–306.

———, AND D. A. SARAVANOS. 1995. Exact free vibration analysis of laminated plates with embedded piezoelectric layers. J. Acoust. Soc. Am. 98:1547–1557.

———, G. RAMIREZ, AND D. A. SARAVANOS. 1994. Coupled discrete-layer finite element models for laminated piezoelectric plates. Comm. Numerical Methods in Eng. 10:971–981.

HYER, M. W. 1998. Stress analysis of fiber-reinforced composite materials. WCB/McGraw-Hill, Boston, MA.

IRUDAYARAJ, J. K., K. HAGHIGHI, AND R. L. STROSHINE. 1990. Nonlinear finite element analysis of coupled heat and mass transfer problems with an application to timber drying. Drying Technol. 8(4):731–749.

JONES, R. M. 1975. Mechanics of composite materials. McGraw-Hill, New York, NY.

KNUFFEL, W., AND A. PIZZI. 1986. The piezoelectric effect in structural timber. Holzforschung 40:157–162.

LANG, E. M., J. R. LOFERSKI, AND J. D. DOLAN. 1995. Hygroscopic deformation of wood-based composite panels. Forest Prod. J. 45(3):67–70.

LEE, H. J., AND D. A. SARAVANOS. 1997. Generalized finite element formulation for smart multilayered thermal piezoelectric composite plates. Int. J. Solids Struct. 34(26):3355–3371.

MASON, W. P. 1950. Piezoelectric crystals and their application to ultrasonics. D. Van Nostrand, New York, NY.

MCMILLEN, J. 1955. Drying stresses in red oak. Forest Prod. J. 5(1):71–76.

MINDLIN, R. D. 1974. Equations of high frequency vibrations of thermopiezoelectric crystal plates. Int. J. of Solids Struct. 10(6):625–637.

MORGAN, K., H. R. THOMAS, AND R. W. LEWIS. 1982. Numerical modeling of stress reversal in timber drying. Wood Sci. 15(2):139–149.

MOUGEL, E., A. L. BERALDO, AND Z. ZOULALIAN. 1995. Controlled dimensional variations of a wood-cement composite. Holzforschung 49:471–479.

NOWACKI, W. 1975. Dynamic problems of thermoelasticity. Noordhoff International Publishing, Leyden, The Netherlands.

PAGANO, N. J. 1970. Exact solutions for rectangular bidirectional composites and sandwich plates. J. Composite Mater. 4:20–34.

PAULEY, K. E., AND S. B. DONG. 1976. Analysis of plane waves in laminated piezoelectric plates. Wave Electronics 1:265–285.

PLUMB, O. A., C. A. BROWN, AND B. A. OLMSTEAD. 1984. Experimental measurements of heat and mass transfer during convective drying of southern pine. Wood Sci. Technol. 18:187–204.

RAY, M. C., R. BHATTACHARYA, AND B. SAMATA. 1993. Exact solutions for static analysis of intelligent structures. AIAA J. 31:1684–1691.

REDDY, J. N. 1987. A generalization of two-dimensional theories of laminated composite plates. Communications in Appl. Numerical Methods 3:173–180.

———. 1989. On the generalization of displacement-based laminate theories. Appl. Mechanics Rev. 42(11) Part 2:S213–S222.

———. 1993. An introduction to the finite element method, 2nd ed. McGraw-Hill, New York, NY.

———. 1997. Mechanics of laminated composite plates: theory and analysis. CRC Press, Boca Raton, FL.

RODGERS, O. E. 1991. Effect on plate frequencies of local wood removal from violin plates supported at the edges. CAS Journal. 1:7–18.

SARAVANOS, D. A., P. R. HEYLIGER, AND D. A. HOPKINS. 1997. Layerwise mechanics and finite element for the dynamic analysis of piezoelectric composite plates. Int. J. Solids Struct. 34(3):359–378.

SCHUMACHER, R. 1988. Compliances of wood for violin top plates. J. Acoust. Soc. Am. 84:1223–1228.

SHARP, D. 1994. Composite structural wood products–manufacturing and application. J. Inst. Wood Sci. 13: 442–446.

SIAU, J. F. 1984. Transport processes in wood. Springer-Verlag, Berlin Heidelberg, Germany.

SIH, G. C., J. G. MICHOPOULOS, AND S. C. CHOU. 1986. Hygrothermoelasticity. Martinus Nijhoff, Dordrecht, The Netherlands.

SIMPSON, W. T. 1973. Predicting equilibrium moisture content of wood by mathematical models. Wood Fiber 5(1): 41–49.

SKAAR, C. 1988. Wood-water relations. Springer-Verlag, New York, NY.

SMITTAKORN, W., AND P. R. HEYLIGER. 2000. A discrete-layer model of laminated hygrothermopiezoelectric plates. Mech. Composite Maters. Struc. 7:79–104.

TAUCHERT, T. R. 1992. Piezothermoelastic behavior of a laminated plate. J. Thermal Stresses 15:25–37.

THOMAS, H. R., R. W. LEWIS, AND K. MORGAN. 1980. An application of the finite element method to the drying of timber. Wood Fiber 11(4):237–243.

TREMBLAY, C., A. CLOUTIER, AND B. GRANDJEAN. 1999. Experimental determination of the ratio of vapor diffusion to the total water movement in wood during drying. Wood Fiber Sci. 31(3):235–248.

TSOUMIS, G. T. 1991. Science and technology of wood: structure, properties, utilization. Van Nostrand Reinhold, New York, NY.

VOIGHT, W. 1928. Lehrbuch der Kristallphysik, 2nd ed. B. G. Teubner, Leipzig, Germany.

WHITNEY, J. M., AND J. E. ASHTON. 1971. Effect of environment on the elastic response of layered composite plates. Am. Inst. Aeronautics Astronautics J. 9:1708–1713.

XU, D., AND O. SUCHSLAND. 1996. A modified elastic approach to the theoretical determination of the hygroscopic warping of laminated wood panels. Wood Fiber Sci. 28(2):194–204.

XU, K., A. K. NOOR, AND Y. Y. TANG. 1995. Three-dimensional solutions for coupled thermoelectroelastic response of multilayered plates. Computer Methods Appl. Mech. Eng. 126:355–371.